GMR Genetics and Molecular Research
Online Journal
ISSN:1676-5680

Molecular cloning, characterization, and bioactivity analysis of interleukin 18 in giant panda (*Ailuropoda melanoleuca*)

Y. Yan[1]*, Q. Wang[2]*, L.L. Niu[2], J.B. Deng[2], J.Q. Yu[2], Y.Z. Zhang[1], J.X. Wang[1], M.M. Yin[1] and X.M. Tan[1]

[1]Key Laboratory for Bio-Resources and Eco-Environment of Ministry of Education, College of Life Sciences, Sichuan University, Chengdu, China
[2]Chengdu Zoo, Chengdu, China

*These authors contributed equally to this study.
Corresponding author: X.M. Tan
E-mail: txmyyf@scu.edu.cn

Genet. Mol. Res. 13 (4): 9687-9700 (2014)
Received January 6, 2014
Accepted May 29, 2014
Published November 19, 2014
DOI http://dx.doi.org/10.4238/2014.November.19.1

ABSTRACT. Interleukin 18 (IL-18), as a member of IL-1 superfamily, is an important pleiotropic cytokine that modulates Th1 immune responses. In this report, we cloned and identified a homolog of IL-18 in giant panda (*Ailuropoda melanoleuca*) (designated as AmIL-18) from peripheral blood mononuclear cells stimulated with lipopolysaccharide. The open reading frame of *AmIL-18* cDNA is 579 bp encoding a deduced protein of 192 amino acids. *AmIL-18* gDNA fragments contained 5 exons and 4 introns. The amino acid sequence of AmIL-18 shared 23.9 to 87.0% identity with other species. To evaluate the effects of AmIL-18 on the immune response, we expressed the recombinant AmIL-18 in *Escherichia coli* BL21 (DE3). The fusion protein PET-AmIL-18 was purified by nickel affinity column chromatography and verified by sodium dodecyl sulfate polyacrylamide gel electrophoresis and Western blot analysis. The biological function of purified PET-AmIL-18 was determined

on mouse splenocytes by quantitative real-time polymerase chain reaction. INF-γ and other cytokines were increased when stimulated by PET-AmIL-18, particularly when combined with recombinant human interleukin 12, while a Th2-type cytokine, interleukin-4, was strikingly suppressed. These results will provide information for the potential use of recombinant proteins to manipulate the immune response in giant pandas and facilitate the study to protect this treasured species.

Key words: Giant panda; Interleukin 18; Molecular cloning; Bioactivity analysis

INTRODUCTION

Interleukin 18 (IL-18) was originally named gamma interferon (IFN-γ) inducing factor (IGIF), and it is an endotoxin-induced serum active substance (Nakamura et al., 1989). IL-18 can induce a high level secretion of IFN-γ in mice treated with *Propionibacterium acnes* challenged with lipopolysaccharide (LPS) (Okamura et al., 1995).

Human IL-18 contains a 193-amino acid precursor peptide (Ushio et al., 1996) and is produced in macrophages, dendritic cells, keratinocytes, Kupffer cells, microglial cells, synovial fibroblasts, and intestinal epithelial cells (Stoll et al., 1998). Although IL-18 shares little sequence similarity with other cytokines, it still belongs to the IL-1 family based on its structure. Similar to IL-1β, IL-18 is first synthesized as an inactive precursor peptide and is cleaved by caspase-1 (interleukin-1β-converting enzyme) to a mature and bioactive form for secretion (Gu et al., 1997).

IL-18 is a pleiotropic effect cytokine in the innate and acquired immune responses to pathogens. Functionally, it is supposed to be similar to IL-12, and both can induce IFN-γ and are involved in rheumatoid arthritis. In addition, IL-18 and IL-12 synergize for IFN-γ production in Th1 cells (Yoshimoto et al., 1998). Besides, they act as a co-inducer to enhance the production of IL-13 in NK cells and T lymphocytes (Hoshino et al., 1999).

IL-18 also possesses several unique features, including its ability to enhance NK-T and NK cell maturation and cytotoxicity (Dao et al., 1998), increase Fas/FasL-dependent cytotoxicity, and potentially induce IgE, IgG1, and Th2 cytokines in murine experimental models (Hoshino et al., 2001). Moreover, IL-18 is involved in the differentiation of Th17 cells by synergistically acting with IL-23 (Weaver et al., 2006). IL-18 can enhance the efficacy of vaccines in immune response to bacteria, viruses, and parasites. Hence, it may be clinically applicable as an antimicrobial and antitumor agent. Recently, it has been shown that IL-18 can inhibit the replication of many viruses such as influenza virus and porcine reproductive and respiratory syndrome virus (Chen et al., 2009).

The giant panda (*Ailuropoda melanoleuca*), as one of the most endangered animals, may have emerged originally in the Late Miocene times (800 million years ago). This archaic species is also considered to be a living fossil. Its survival mainly spread in the mountains of Sichuan, Shaanxi, and Gansu in China (Wei et al., 2012). The Third National Survey revealed that there were 1596 individuals in the wild, and a molecular census estimate showed that this quantity might be 2500 to 3000 (Zhan et al., 2006). In the past decades, the shrinking of giant panda populations was caused by lost and broken habitats (Shen et al., 2008), low fertility, and

susceptibility to infectious diseases. A study confirmed that canine distemper virus, canine parvovirus, canine coronavirus, and canine adeno virus threaten the giant pandas (Qin et al., 2010). Consequently, it is essential to study the immune system of giant panda, especially immune function genes.

The giant panda genome has been sequenced and assembled using next-generation sequencing technology. More than 90% of the whole genome was covered (Li et al., 2010). It is convenient and accurate to search for a target gene using this sequence database.

Previous research about IL-18 mainly focused on mammalian and avian species, such as human, mouse, and chicken, but little was known about giant panda. Here, we reported the cDNA and gDNA cloning, gene structure, and phylogenetic analysis of giant panda *IL-18* (*AmIL-18*). In addition, we investigated whether *AmIL-18* could be induced by LPS from peripheral blood mononuclear cells (PBMCs) and whether the soluble recombinant AmIL-18 fusion protein could be produced by *Escherichia coli*. This protein was demonstrated to increase inflammatory response cytokines in mouse spleen cells. These results could provide new therapy option for infectious diseases in giant pandas.

MATERIAL AND METHODS

Animals

The giant panda was bred in Chengdu Zoo (Chengdu, Sichuan, China). Female C57BL/6J mice (6-8 weeks old) were obtained from the Animal Center of Sichuan University. All the animal experimental protocols were approved by the Review Committee for the Use of Human or Animal Subjects of Sichuan University.

Total RNA isolation and cDNA synthesis

The blood was phlebotomized from a captive giant panda. PMBCs were separated by density gradient centrifugation using Histopaque®-1077 (Sigma-Aldrich, MO, USA). Cells (5×10^6) were grown in RPMI 1640 medium with 10% heat-inactivated fetal bovine serum (FBS), penicillin, streptomycin, l-glutamine, and HEPES buffer (Gibco, USA) in the presence of 10 µg/mL LPS (Sigma-Aldrich) for 24 h at 37°C with 5% CO_2.

Total RNA from cultured mononuclear cells was extracted with TRIzol reagent (Invitrogen, CA, USA) according to manufacturer instructions and stored at -80°C. Remaining DNA was removed by DNaseI (Fermentas, Canada). Total RNA (1 µg), $Oligo(dT)_{18}$ (Table 1), and M-MLV reverse transcriptase (Invitrogen) were used in cDNA synthesis.

Cloning and sequencing of *AmIL-18*

The giant panda *IL-18* sequence was investigated by nucleotide basic local alignment search tool (BLAST) (ftp://ftp.ncbi.nlm.nih.gov/blast/) using the giant panda genome on the Giant Panda Database (http://panda.genomics.org.cn/page/panda/index.jsp) assembly version AilMel 1.0 (Li et al., 2010) by alignment with other mammal *IL-18* sequences, including human, mouse, dog, and cat. A fragment located in scaffold 11 was identified to be the potential *IL-18* sequence. Reverse transcription polymerase chain reaction (PCR) was performed with Taq DNA polymerase (TaKaRa, Dalian, China) under conditions of pre-denaturation at 94°C

for 2 min; 30 cycles of denaturation at 94°C for 30 s, annealing at 55°C for 30 s, and extension at 72°C for 1 min; and a final 10-min extension at 72°C. The PCR product was analyzed and recovered from a 1.5% agarose gel using gel extraction kit (Omega, GA, USA).

The products were ligated to the pMD18-T vector (TaKaRa, Dalian, China) and transformed into *E. coli* JM109 competent cells. The bacteria were grown on Luria-Bertani (LB) plates with ampicillin, isopropyl β-D-1-thiogalactopyranoside (IPTG) and 5-bromo-4-chloro-3-indolyl-β-D-galactopyranoside. The positive clones that were selected by blue-white screening were sequenced and named pMD-AmIL18.

Cloning of *AmIL18* genomic DNA

Genomic DNA was isolated from a liver sample of a dead giant panda using a universal genomic DNA extraction kit (TaKaRa, Dalian, China) and stored at -20°C until use. Using genomic DNA as template, PCR was performed under the same conditions as above to obtain the gDNA fragments of *AmIL18* (Table 1). The products were ligated into the pBackZero-T vector (TaKaRa, Dalian, China), and the positive clones were sequenced.

Table 1. Primers used for cloning and quantitative real-time polymerase chain reaction (qRT-PCR) analyses.

Gene name	Primer name	Sequence (5'-3')	Application
Panda			
IL-18 ORF	Am18ORF-F	ATGGCTGCTAACACAGAAGACAATTGC	PCR for cloning cDNA
	Am18ORF-R	CTAGCTTTTGTTTTGAACAGTGAACAT	
IL-18 genomic	Am18GE-1F	*TTTAA*ATGACAGGCATCCTTTACTCACG	PCR for cloning genomic DNA
	Am18GE-1R	*TTTAA*TTTAATAAGCCACATAGCCACCC	
	Am18GE-2F	*TTTAA*GATACTGCCTGGTGATGTTGGG	
	Am18GE-2R	*TTTAA*TGACGGTGAAGGGATTGGTG	
	Am18GE-3F	*TTTAA*GTGACAAATACTTCTTCCCGTTCT	
	Am18GE-3R	*TTTAA*AGAGTCCACAGGTCAGGCTTAT	
	Am18GE-4F	*TTTAA*TAGCCATCGCCTTCCAGC	
	Am18GE-4R	*TTTAA*CTACCCAGGTGCCCGTTATTC	
IL-18 PET	Am18PET-F	CGCGGATCCTACTTTGGCAAGCTCGAACCTAAACTC	PCR for vector construction
	Am18PET-R	CCCAAGCTTCTAGCTTTTGTTTTGAACAGTGAACATAATGG	
Mouse			
GAPDH	MuGAPDH-F	TGCCCAGAACATCATCCCT	qRT-PCR
	MuGAPDH-R	GGTCCTCAGTGTAGCCCAAG	
IFN-γ	MuIFN-γ-F	ACTCAAGTGGCATAGATGTGGAAG	qRT-PCR
	MuIFN-γ-R	TGCTGATGGCCTGATTGTCTT	
IL-4	MuIL-4-F	AACGAGGTCACAGGAGAA	qRT-PCR
	MuIL-4-R	CCTTGGAAGCCCTACAGA	
TNF-α	MuTNF-α-F	GCCACCACGCTCTTCTGTCTACTG	qRT-PCR
	MuTNF-α-R	GTGGGCTACAGGCTTGTCACTCG	
GM-CSF	MuGM-CSF-F	TGCCTGTCACGTTGAATGAAGAG	qRT-PCR
	MuGM-CSF-R	CTGGTAGTAGCTGGCTGTCATGTTC	

Restriction enzyme sites are underlined. *TTTAA* sequence was used for directed cloning.

Sequence analysis

The sequence similarity were analyzed using the BLASTN suite from the National Center for Biotechnology Information (http://blast.ncbi.nlm.nih.gov/) (Altschul et al., 1990). The multiple alignments of deduced amino acids were created using the Clustal Omega (http://www.ebi.ac.uk/Tools/msa/clustalo/) (Larkin et al., 2007) and DNAMAN5.2 software, and then they were edited with the BioEdit program. Post-translational modifications and signal

peptide were predicted by NetNGlyc (ver1.0c) and SignalP (ver4.1) (Julenius et al., 2005; Petersen et al., 2011). The secondary structure was estimated by the YASPIN server based on the NR database for PSI-BLAST (http://www.ibi.vu.nl/programs/yaspinwww/) (Lin et al., 2005). The domain architectures were identified by the simple modular architecture research tool (SMART) (http://smart.embl-heidelberg.de/) (Letunic et al., 2012). The phylogenetic tree of amino acid sequences was constructed using the neighbor-joining method (Saitou and Nei, 1987) by the MEGA program version 5.2 (http://www.megasoftware.net/) (Tamura et al., 2011). The phylogenetic tree was tested with 1000 bootstrap replications. The sequences used for multiple alignments were obtained from the GenBank database (Table 2).

Expression and purification of AmIL-18

cDNA fragment of the mature AmIL-18 was amplified with primers shown in Table 1 and digested with restriction endonucleases *Bam*HI and *Hin*dIII (Fermentas, Canada). It was subcloned into vector pET-32a(+) (Novagen, USA) to construct prokaryotic expression plasmid pET-Am-IL18. The resulting recombinant plasmid was transformed into *E. coli* BL21 (DE3) and was sequenced for validation. Bacteria were grown on LB plates containing 100 μg/mL ampicillin at 37°C. A single colony was shaken in 4 mL LB medium with ampicillin overnight. The culture was transferred to fresh LB medium and continued shaking at 150 rpm and 37°C for about 2-3 h until the optical density at 600 nm (OD_{600}) reached 0.6. The expression was induced with 0.5 mM IPTG (TaKaRa, Dalian, China) for 16 h at 18°C. The bacteria were harvested by centrifugation at 4000 *g* for 10 min, and the pellet was suspended in 20 mM Tris-HCl buffer, pH 8.0. The cell suspension was subjected to sonication with a 3-s burst and 10-s pause for 20 min in a cooling bath. The lysate was clarified by centrifugation at 10,000 *g* for 15 min at 4°C, and the supernatant was collected. For purification, the protein and all buffers were passed through 0.45-μm filters (Merck Millipore, Germany). Histidine-tagged fusion protein was purified on nickel affinity HisTrap HP columns (GE Healthcare, Sweden) by the ÄKTA primer system. After equilibrating the column with binding buffer (20mM Tris-HCl, 0.5 M NaCl, 45 mM imidazole, pH 8.0), the supernatant was loaded onto the column at 1 min/mL. The fusion protein was finally eluted with an elution buffer (20 mM Tris-HCl, 300 mM imidazole, pH 8.0) using linear gradient methods. The concentration was determined using a BCA Protein Assay kit (Thermo Scientific, USA). Then, the purified protein was named PET-AmIL-18 and stored at 4°C with Protease Inhibitor Cocktail (Sigma-Aldrich).

Sodium dodecyl sulfate polyacrylamide gel electrophoresis (SDS-PAGE) and Western blot

The lysate supernatant and purified fusion proteins were separated by 12% SDS-PAGE. Coomassie brilliant blue R-250 (Amresco, USA) was used for visualization. For immunoblot, proteins were transferred to a 0.45-μm hydrophobic polyvinylidene fluoride membrane (Merck Millipore, Germany). The membrane was blocked with Tris-buffered saline with Tween-20 (TBS-T) buffer (20 mM Tris-HCl, 150 mM NaCl, 0.05% Tween-20, pH 8.0) containing 5% skim milk for 12 h at 4°C. The blots were incubated with anti-human IL-18 rabbit polycolonal antibody (Abcam, Britain) which was at diluted 1:2000 in TBS-T buffer. After washing 3 times with TBS-T buffer, the membranes were incubated with 1:20,000 peroxidase conjugated goat anti-rabbit IgG (Thermo Scientific, USA) in TBS-T buffer. The membrane

was incubated with Amersham™ ECL™ select Western blotting detection reagent (GE Healthcare, Sweden). Blots were visualized by X-ray film.

Biological activity analysis

The biological function of purified PET-AmIL-18 was examined according to its effect on the expression of potential cytokine-responsive genes, such as *IFN-γ*, *IL-4*, *TNF-α* and *GM-CSF*.

Mouse splenocytes were separated, and 1 x 10^6 cells/well were cultured on 24-well plates in RPMI-1640 with 10% FBS in triplicate. Then, groups were treated with PET-AmIL-18 (500 ng/mL), PET-AmIL-18 (500 ng/mL)/recombinant human IL-12 (1 ng/mL, Peprotech, USA), and phosphate-buffered saline (PBS) as a control. All cells were incubated for 24 h at 37°C in 5% CO_2.

Total RNA was isolated from the cultured spleen lymphocytes using TRIzol reagent. cDNA synthesis and contaminative genomic DNA removal were performed by PrimeScript™ RT Reagent Kit with gDNA Eraser (TaKaRa, Dalian, China). Reverse transcription was performed at 37°C for 15 min and 85°C for 5 s.

The primers to detect the transcripts of mouse *IFN-γ* (NM_008337.3), *IL-4* (NM_021283.2), *TNF-α* (NM_013693.2), *GM-CSF* (NM_009969.4), and the housekeeping gene control *GAPDH* (NM_008084.2) were designed using Beacon Designer ver7.92 and Primer Premier ver5.0 (Table 1). Quantitative real-time PCR (qRT-PCR) was performed with KOD SYBR® qPCR Mix (TOYOBO, Japan) using a CFX Connect™ Real-Time PCR Detection System (Bio-Rad, CA, USA). The standard curves were established by calculating cycle thresholds (Ct) of 5 dilutions of cDNA to verify the efficiency of the primer pairs. A 20-μL reaction was composed of 1 μL diluted cDNA, 0.4 μL 10 mM each primer, 10 μL KOD SYBR® qPCR Mix, and DNase-free water. The PCR was performed with the following program: 98°C for 2 min; 40 cycles of 98°C for 10 s, 60°C (depends on primer melting temperature) for 10 s, and 68°C for 30 s. The relative expression level of these transcripts were normalized to the expression level of *GAPDH* control using Bio-Rad CFX Manager and were calculated using the $2^{-\Delta\Delta Ct}$ methods (Livak and Schmittgen, 2001). Data in response to different media were converted to the fold expression relative to that of the PBS controls. Statistical analysis of the data was conducted using the SPSS 13 software; one-way analysis of variance was employed to evaluate the statistical differences among groups. $P < 0.05$ was considered to be statistically significant.

RESULTS

Sequence analysis of the *AmIL-18* gene

The open reading frame (ORF) of the *AmIL-18* is 579 bp in length and encodes 192 amino acid residues (GenBank accession No. HQ874655.1). No typical signal peptide was found on AmIL-18. However, like other known IL-1 family members, it has a leader peptide of 35 amino acids that is followed by a mature peptide of 158 amino acids. A conserved caspase-1 cut site, Asp^{35}-Tyr^{36}, was determined by multiple sequence alignment with other IL-18 proteins of several animals. NetNGlyc Servers revealed that it contains an N-glycosylation site on N^{113}-KTI^{116}, but no O-glycosylation site was found. Ten serine and 1 tyrosine residue were potential kinase-specific phosphorylation sites.

The secondary structure predicted by YASPIN and the structure of human IL-18 (Kato

et al., 2003) indicated that AmIL-18 is composed of 12 β-strands and 3 α-helices (Figure 1).

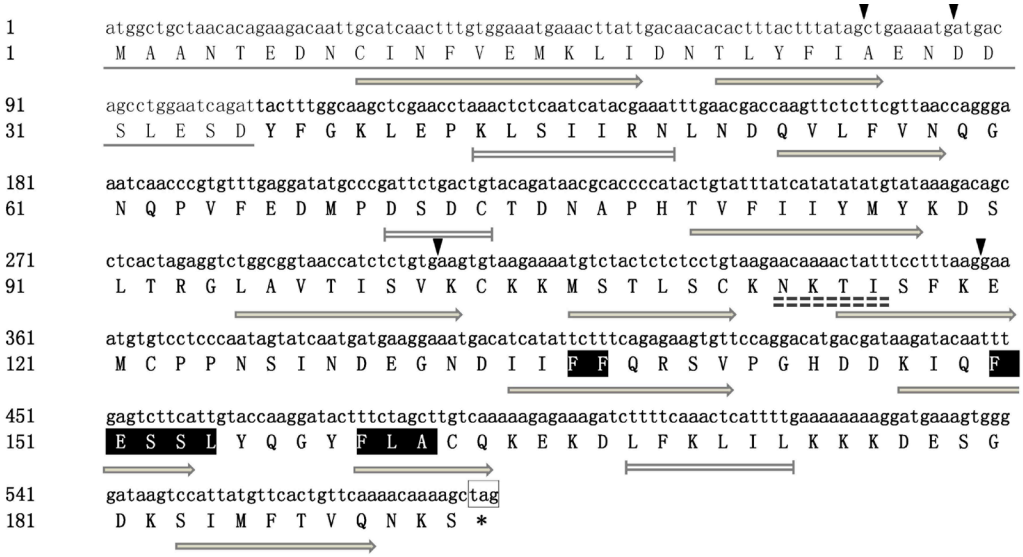

Figure 1. Full-length cDNA and deduced amino acid sequences of giant panda IL-18. The leading peptide is underlined and the stop codon is boxed. The predicted secondary structures are indicated by horizontal arrows (β-strand) and double solid lines (α-helix). Four vertical triangles represent the exon/intron splice site. The possible N-glycosylation site is dotted underlined. The conserved domain residues of the IL-18 family structure are shaded.

Cloning of panda *IL-18* genomic DNA

The genomic DNA fragment of *AmIL-18* spaned 10,400 bp (GenBank accession No. KF512471) and was located on genome scaffold 11. The orthologous gene was on human chromosome 11 (11q22.2-q22.3) and chicken chromosome 24. The genes *PTS*, *BCO2*, *TEX12*, *SDHD*, *TIMM8B*, and *C11orf57* appeared on both sides of *IL-18* with the same orientation except that *TIMM8B* was deleted in chicken (Figure 2A).

A comparison of the *AmIL-18* genomic DNA sequence and cDNA sequence demonstrates that it contained 5 exons and 4 introns. The gene is spliced following GT/AG rule at the 5' and 3' ends of the introns. The length and structure of *AmIL-18* gene are approximately the same as those of the human gene (11.4 kb).

The genomic organization of the *IL-18* gene of giant panda and other vertebrates was determined. *IL-18* genes in mammals and birds contained 5 exons and 4 introns (Figure 2B). Most species had an analogous exon distribution, but the introns varied in length.

Multiple alignment of IL-18

Multiple sequence alignments with other known IL-18 amino acid sequences revealed that AmIL-18 shared high protein identity with mammalian IL-18 (62.8-87.0%), moderate identity with birds (31.7-33.2%), and low identity with amphibians and fish (23.9-25.8%) (Table 2).

Like the IL-1 family signature pattern (Bird et al., 2002), there is also a conserved domain in the C terminus of AmIL-18 and other IL-18s (Figure 3). The conserved motif L^{32}-E-S-D^{35} acts as a caspase-1 cleavage site. Besides, D^{67}-M-P-D^{70} and D^{72}-C-T-D^{75} motifs were recognition sites for caspase-3.

Molecular evolutionary analysis of the IL-18 sequence was conducted using the neighbor-joining method. As shown in the phylogenetic tree (Figure 4), AmIL-18 was in the branch of mammalian IL-18, close to that of dog and cat.

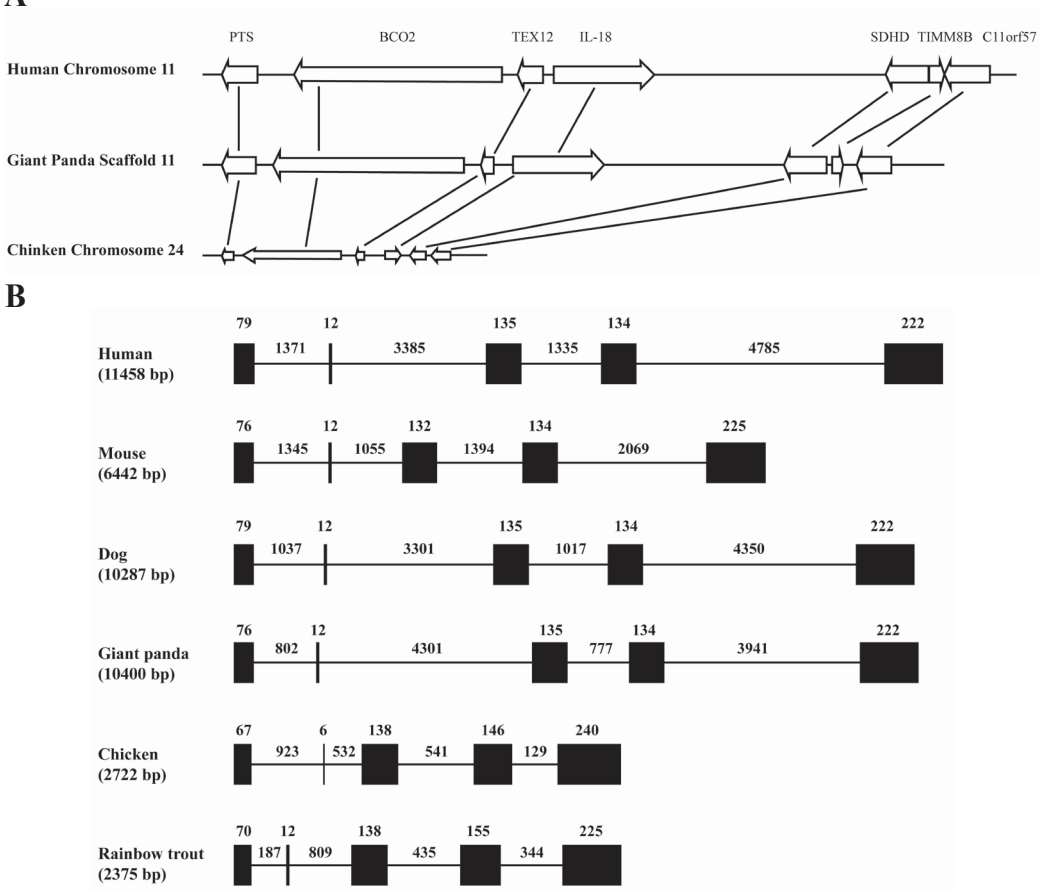

Figure 2. *IL-18* gene organization. **A.** Comparison of the human, panda, and chicken *IL-18* locus on the chromosome. Arrows represent the gene length and orientation. **B.** Schematic comparing *IL-18* gene exon location and size among human, mouse, dog, panda, chicken, and rainbow trout. Black boxes indicate the regions of the exons and lines between boxes represent the intron regions. The sizes are indicated above each region.

Expression and purification of AmIL-18 protein

The sequence encoding the mature peptide was successfully inserted into the pET-32a vector. After being transformed into *E. coli* BL21 (DE3) and induced by IPTG, the supernatant of the cell lysate was visualized by SDS-PAGE. Compared with control BL21 (DE3) cells and

non-induced cells harboring pET-AmIL18, a fusion protein with a molecular weight of 35.7 kDa was expressed in soluble form. The supernatant was applied to the Ni Sepharose column and purified using the Histidine-6 tag peptide at the N-terminus. After elution, a single band was displayed on the gel (Figure 5). The concentration of the purified PET-AmIL-18 was approximately 0.5 mg/mL according to the bicinchoninic acid method. To confirm this band as the AmIL-18 fusion protein, anti-human IL18 polyclonal antibody was used in Western blot. The protein was recognized by anti-IL18 polyclonal antibody and a corresponding second antibody, whereas no band appeared in the control lane (Figure 5).

Table 2. Percent identity of IL-18 amino acid sequences from different animals.

Species	Common name	Accession No.	Nucleotide (bp)	Precursor (aa)	Mature (aa)[a]	Identity (%)
Homo sapiens	Human	NP_001553.1	582	193	157	76.56
Mus musculus	Mouse	NP_032386.1	579	192	157	65.08
Rattus norvegicus	Rat	NP_062038.1	585	194	158	62.83
Sus scrofa	Pig	NP_999162.1	579	192	157	86.98
Canis lupus familiaris	Dog	NP_001003169.1	582	193	157	85.94
Equus caballus	Horse	NP_001075981.1	582	193	157	85.94
Bos taurus	Cattle	NP_776516.1	582	193	157	80.73
Ovis aries	Sheep	NP_001009263.1	582	193	157	81.77
Felis catus	Cat	NP_001009213.2	579	192	157	84.90
Macaca mulatta	Monkey	NP_001028006.1	582	193	157	75.52
Oryctolagus cuniculus	Rabbit	NP_001116412.1	579	192	157	74.48
Gallus gallus	Chicken	NP_989939.1	597	198	169	33.15
Meleagris gallopavo	Turkey	XP_003212805.1	597	198	169	32.60
Taeniopygia guttata	Zebra finch	XP_002189810.2	576	191	161	32.96
Anas platyrhynchos	Mallard	ABF69034.1	603	200	170	31.69
Anolis carolinensis	Green anole	XP_003229579.1	606	201	169	25.81
Xenopus tropicalis	Clawed frog	XP_002942520.1	627	208	NC[b]	23.89
Atlantic salmon	Salmo salar	NP_001134880.1	621	206	NC	28.89
Takifugu rubripes	Fugu rubripes	NP_001027804.1	558	185	158	26.67
Oncorhynchus mykiss	Rainbow trout	NP_001118089.1	600	199	167	29.61
Ailuropoda melanoleuca	Giant panda	HQ874655.1	579	192	157	-

[a]Mature peptide length was predicted using the conserved caspase-1 cleavage site. [b]NC, no clear conserved caspase-1 cleavage site.

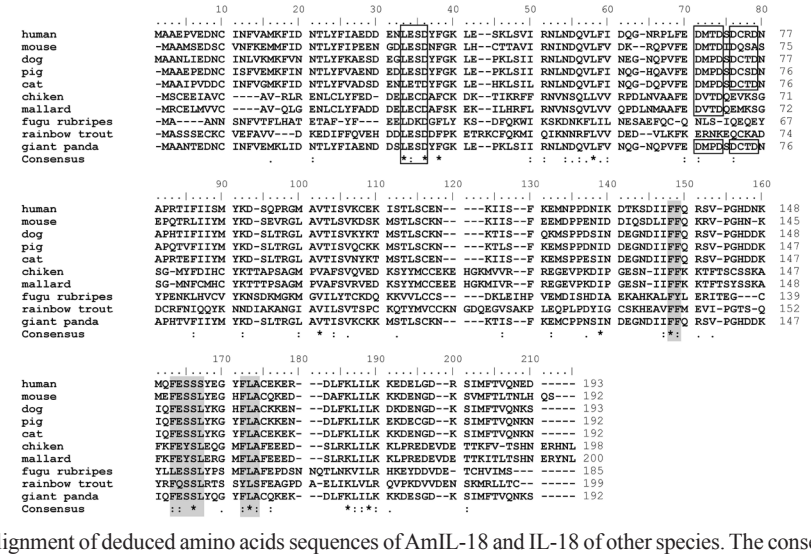

Figure 3. Alignment of deduced amino acids sequences of AmIL-18 and IL-18 of other species. The conserved domain residues of the IL-18 family structure are shaded. The conserved caspase-1 and caspase-3 cleavage sites are boxed.

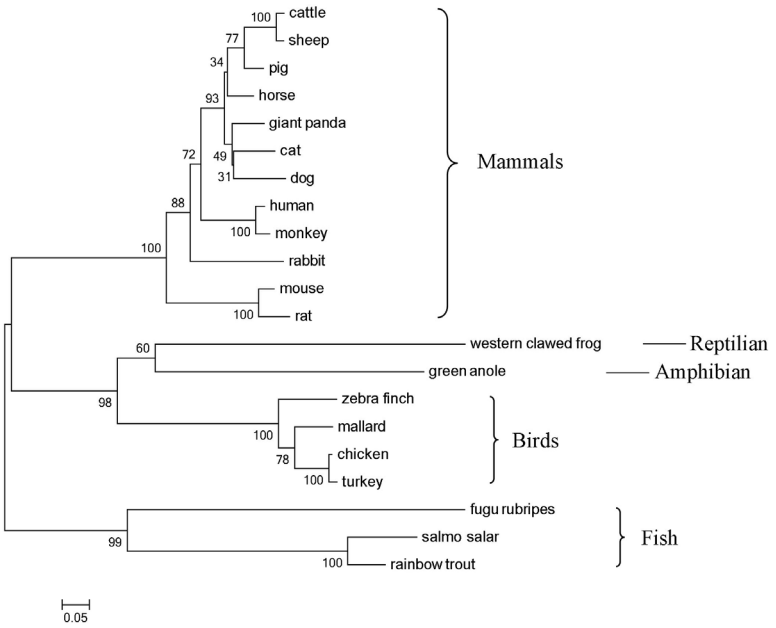

Figure 4. Phylogenetic tree based on different IL-18 molecules. The bootstrap consensus tree was constructed using the neighbor-joining algorithm by MEGA. The node number is the bootstrap confidence derived from 1000 replications. The scale bar was 0.05. The sequence accession numbers are listed in Table 2.

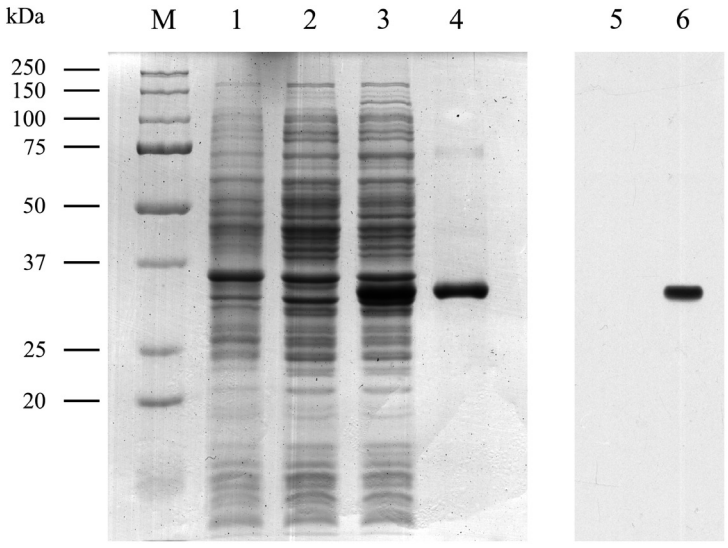

Figure 5. PET-AmIL-18 fusion protein expression and purification in *Escherichia coli* BL21 (DE3). *Lane M* = molecular weight marker; *lane 1* = cell lysates of *Escherichia coli* BL21 (DE3); *lane 2* = cell lysates of bacteria harboring pET-AmIL18 without isopropyl β-D-1-thiogalactopyranoside (IPTG) induction; *lane 3* = cell lysates of bacteria harboring pET-AmIL18 with 0.5 mM IPTG induction; *lane 4* = purified PET-AmIL-18 fusion protein; *lane 5* = Western blot analysis of cell lysates of *E. coli* BL21 (DE3); *lane 6* = Western blot analysis of cell lysates of bacteria harboring pET-AmIL18 with IPTG induction: the band corresponding to the induced PET-AmIL-18 protein.

Bioactivity of AmIL-18

To determine the biological activity of AmIL-18, mouse spleen lymphocytes were treated with recombinant proteins. The effect on cytokine production was measured by qRT-PCR. As shown in Figure 6, together with hIL-12, PET-AmIL-18 significantly induced mouse lymphocyte *IFN-γ* mRNA expression about 24-fold higher than that of the PBS control, whereas PET-AmIL-18 alone induced a 9-fold increase. The level of *TNF-α* and *GM-CSF* mRNA in the mouse lymphocytes was increased when cells were incubated with PET-AmIL-18 and hIL-12. However, with the same treatment, the *IL-4* expression was remarkably suppressed, only 0.5-fold in the PET-AmIL-18 treatment compared with the control.

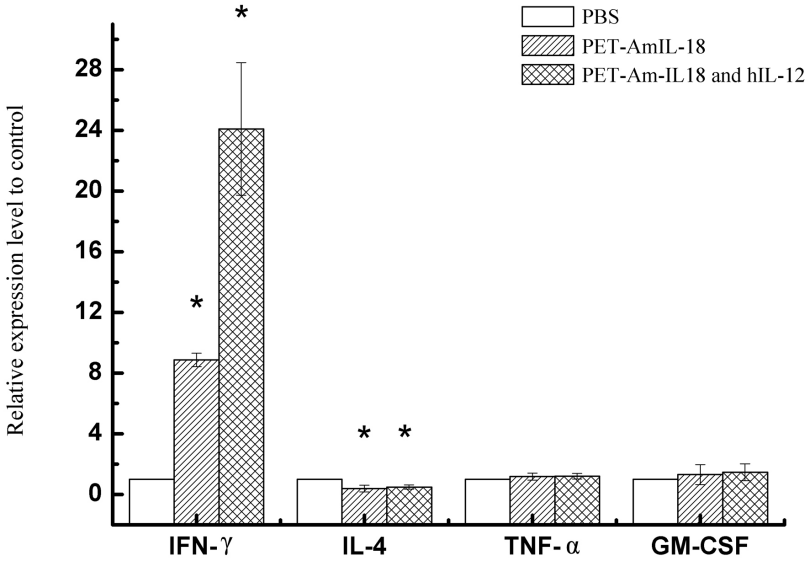

Figure 6. Biological effect of PET-AmIL-18 in mouse lymphocytes. The mean mRNA levels of *IFN-γ*, *IL-4*, *TNF-α*, and *GM-CSF* were measured by quantitative real-time polymerase chain reaction. Relative expression data were calculated by the $2^{-\Delta\Delta Ct}$ method compared to the phosphate-buffered saline (PBS) control (set to 1). *Significant difference by the *t*-test ($P < 0.05$).

DISCUSSION

In this study, we isolated and characterized the *IL-18* gene in giant panda, and we reported the biological activity of the recombinant PET-AmIL-18 protein on lymphocytes. The *IL-18* transcripts were acquired from various tissues and organs, including the spleen, peripheral blood, and some non-immune tissues. In this experiment, a peripheral blood sampling method was adopted as a safe way to obtain the precious samples. Bacterial LPS always acts as an effective exogenous stimulator of immunity in eukaryotic species. In this study, *AmIL-18* RNA was transcribed in panda PBMCs post LPS stimulation, whereas no transcript was obtained from non-LPS stimulation (data not shown). Gene fragments were predicted from the giant panda genome database BLAST with other homologous sequences. With more ge-

nome databases being published, these convenient methods will be widely used to search and clone new genes. The predicted AmIL-18 amino acid sequence had identity with other species that ranged from 23.9 to 87.0%. It had the highest homology with pig IL-18 and the lowest homology with clawed frog IL-18. The phylogenetic tree was divided into 3 main branches: mammals, birds, and fish. The clades of giant panda, cat, and dog were clustered together and formed a subgroup, reflecting a close relationship between giant panda and Caniformia, which was consistent with the evolutionary taxonomy (Yu et al., 2011).

Bioinformatic analysis showed a caspase-1 cleavage site in the N-terminal domain, producing a mature peptide by removing the leading peptide (Liu et al., 2000). There is a conserved caspase-1 cleavage motif (L-X-X-D) in most vertebrates (Figure 2), which might be a useful candidate to the generate an effective caspase-1 inhibitor (Denes et al., 2012). The D-X-X-D motif, which is supposed to be a specific action site for caspase-3, was common in mammals but deficient in fish. Glu^{41} and Lys^{88} are conserved amino acid residues that bind the surface IL-18Rα chain involved in the signal transduction and are critical for the integrity of the IL-18 structure (Kim et al., 2002).

Similar to other mammals, the N-glycosylation site was N^{113}-KTI^{116}, and dog, pig, and sheep had another site glycosylated (NN^{20}-TL^{22}). As a member of the IL-1 family (IL-1α, IL-1β, IL-1Ra, IL-33, etc.), IL-18 possessed a conserved region in the C-terminus like the following IL-1β consensus pattern: F-[FY]-X_{11-13}-[FL]-X_2-S-[SL]-X_4-[FY]-L-[SA] (Zou et al., 2004). With more sequence data generation, the unique IL-18 signature needs to be modified to F-[FY]-X_{10-13}-[FL]-[EQ]-[SY]-S-[SL]-X_4-[FY]-L-[AS].

The sequence analysis revealed that AmIL-18 had species-specific differences because there was at least 1 amino acid variation between the sequence of giant panda IL-18 and all the other sequences available. For example, 6 cysteine residues were found at positions 9, 73, 103, 111, 122, and 162, which were different sites than those observed for other species. However, the amino acid substitutions and insertions might not affect the activity of AmIL-18 because the N-glycosylation site and 6 cysteines were intact.

E. coli is the most common prokaryotic expression systems, and it has many advantages, such as low cost, easy to operate, and high yield compared with the cell expression system. For functional characterization of mature AmIL-18, the gene was inserted into the pET32a vector and then expressed in *E. coli* BL21 (DE3). To increase the soluble expression, we tested different inducing conditions, including temperature, time, IPTG concentration, cell OD value, and solution buffer. As a result, the induction under 0.5 mM IPTG at 18°C for 16-20 h were deemed the optimal condition for the fusion protein. Western blot analysis of lysates from the induced bacteria harboring pET-AmIL18 exhibited an expected band at 35.7 kDa, indicating the soluble expression of AmIL-18.

The bioactivity of AmIL-18 was demonstrated by performing an *in vitro* experiment with mouse lymphocytes. The results showed that AmIL-18 produced in *E. coli* was completely active biologically. It could unambiguously increase the expression of *IFN-γ*. In addition, IL-18 and IL-12 had a synergistic effect on the stimulation of T cells to produce IFN-γ (Nakahira et al., 2002). In this study, the expression of *IFN-γ* was significantly increased with PET-AmIL-18 combined with human IL-12 treatment compared with PET-AmIL-18 treatment alone. This demonstrated cytokines from diverse species can interact with each other. Because of the *IFN-γ*-inducing activity of IL-18, it was identified as a good candidate for immune therapy against viruses (Ma et al., 2008).

Previous studies proved that IL-18 also promoted the secretion of cytokines such as *TNF-α*, and *GM-CSF* to promote the proliferation, development, and differentiation of Th1 cells (Kohno and Kurimoto, 1998). Here, the expression of *TNF-α* and *GM-CSF* were increased by incubation with PET-AmIL-18.

In conclusion, we successfully cloned, expressed, and purified of the recombinant giant panda IL-18 protein from *E. coli*. Our data also demonstrated its biological function on mouse lymphocytes. As a member of the IL-1 superfamily, AmIL-18 could induce some inflammatory cytokines. It may be produced in some suitable forms that can be used on giant pandas, such as immunologic adjuvants. These results will facilitate the protection of giant panda according etiology and immunology.

ACKNOWLEDGMENTS

Research supported by Chengdu Research Fund of Giant Panda Breeding.

REFERENCES

Altschul SF, Gish W, Miller W, Myers EW, et al. (1990). Basic local alignment search tool. *J. Mol. Biol*. 215: 403-410.

Bird S, Zou J, Wang TH, Munday B, et al. (2002). Evolution of interleukin-1 beta. *Cytokine Growth Factor Rev*. 13: 483-502.

Chen HY, Zheng LL, Li XS, Wei ZY, et al. (2009). Cloning, *in vitro* expression, and bioactivity of interleukin-18 isolated from a domestic porcine breed found in Henan. *FEMS Immunol. Med. Microbiol*. 57: 129-135.

Dao T, Mehal WZ and Crispe IN (1998). IL-18 augments perforin-dependent cytotoxicity of liver NK-T cells. *J. Immunol*. 161: 2217-2222.

Denes A, Lopez-Castejon G and Brough D (2012). Caspase-1: is IL-1 just the tip of the ICEberg? *Cell Death Dis*. 3:e338.

Gu Y, Kuida K, Tsutsui H, Ku G, et al. (1997). Activation of interferon-gamma inducing factor mediated by interleukin-1 beta converting enzyme. *Science* 275: 206-209.

Hoshino T, Kawase Y, Okamoto M, Yokota K, et al. (2001). Cutting edge: IL-18-transgenic mice: *in vivo* evidence of a broad role for IL-18 in modulating immune function. *J. Immunol*. 166: 7014-7018.

Hoshino T, Wiltrout RH and Young HA (1999). IL-18 is a potent coinducer of IL-13 in NK and T cells: a new potential role for IL-18 in modulating the immune response. *J. Immunol*. 162: 5070-5077.

Julenius K, Mølgaard A, Gupta R and Brunak S (2005). Prediction, conservation analysis, and structural characterization of mammalian mucin-type O-glycosylation sites. *Glycobiology* 15: 153-164.

Kato Z, Jee J, Shikano H, Mishima M, et al. (2003). The structure and binding mode of interleukin-18. *Nat. Struct. Biol*. 10: 966-971.

Kim SH, Azam T, Novick D, Yoon DY, et al. (2002). Identification of amino acid residues critical for biological activity in human interleukin-18. *J. Biol. Chem*. 277: 10998-11003.

Kohno K and Kurimoto M (1998). Interleukin 18, a cytokine which resembles IL-1 structurally and IL-12 functionally but exerts its effect independently of both. *Clin. Immunol. Immunopathol*. 86: 11-15.

Larkin MA, Blackshields G, Brown NP, Chenna R, et al. (2007). Clustal W and Clustal X version 2.0. *Bioinformatics* 23: 2947-2948.

Letunic I, Doerks T and Bork P (2012). SMART 7: recent updates to the protein domain annotation resource. *Nucleic Acids Res*.40: D302-D305.

Li RQ, Fan W, Tian G, Zhu HM, et al. (2010). The sequence and *de novo* assembly of the giant panda genome. *Nature* 463: 311-317.

Lin K, Simossis VA, Taylor WR and Heringa J (2005). A simple and fast secondary structure prediction method using hidden neural networks. *Bioinformatics* 21: 152-159.

Liu BL, Novick D, Kim SH and Rubinstein M (2000). Production of a biologically active human interleukin 18 requires its prior synthesis as pro-IL-18. *Cytokine* 12: 1519-1525.

Livak KJ and Schmittgen TD (2001). Analysis of relative gene expression data using real-time quantitative PCR and the 2 (-Delta Delta C(T) method. *Methods* 25: 402-408.

Ma M, Jin N, Shen G, Zhu G, et al. (2008). Immune responses of swine inoculated with a recombinant fowlpox virus co-

expressing P12A and 3C of FMDV and swine IL-18. *Vet. Immunol. Immunopathol*. 121: 1-7.
Nakahira M, Ahn HJ, Park WR, Gao P, et al. (2002). Synergy of IL-12 and IL-18 for IFN-gamma gene expression: IL-12-induced STAT4 contributes to IFN-gamma promoter activation by upregulating the binding activity of IL-18-induced activator protein 1. *J. Immunol*. 168: 1146-1153.
Nakamura K, Okamura H, Wada M, Nagata K, et al. (1989). Endotoxin-induced serum factor that stimulates gamma interferon production. *Infect. Immun*. 57: 590-595.
Okamura H, Tsutsui H, Komatsu T, Yutsudo M, et al. (1995). Cloning of a new cytokine that induces IFN-gamma production by T cells. *Nature* 378: 88-91.
Petersen TN, Brunak S, von Heijne G and Nielsen H (2011). SignalP 4.0: discriminating signal peptides from transmembrane regions. *Nat. Methods* 8: 785-786.
Qin Q, Li DS, Zhang HM, Hou R, et al. (2010). Serosurvey of selected viruses in captive giant pandas (*Ailuropoda melanoleuca*) in China. *Vet.Microbiol*. 142: 199-204.
Saitou N and Nei M (1987). The neighbor-joining method: a new method for reconstructing phylogenetic trees. *Mol. Biol. Evol*. 4: 406-425.
Shen GZ, Feng CY, Xie ZQ, Ouyang ZY, et al. (2008). Proposed conservation landscape for giant pandas in the Minshan Mountains, China. *Conserv. Biol*. 22: 1144-1153.
Stoll S, Jonuleit H, Schmitt E, Müller G, et al. (1998). Production of functional IL-18 by different subtypes of murine and human dendritic cells (DC): DC-derived IL-18 enhances IL-12-dependent Th1 development. *Eur. J. Immunol*. 28: 3231-3239.
Tamura K, Peterson D, Peterson N, Stecher G, et al. (2011). MEGA5: molecular evolutionary genetics analysis using maximum likelihood, evolutionary distance, and maximum parsimony methods. *Mol. Biol. Evol*. 28: 2731-2739.
Ushio S, Namba M, Okura T, Hattori K, et al. (1996). Cloning of the cDNA for human IFN-gamma-inducing factor, expression in *Escherichia coli*, and studies on the biologic activities of the protein. *J. Immunol*. 156: 4274-4279.
Weaver CT, Harrington LE, Mangan PR, Gavrieli M, et al. (2006). Th17: an effector CD4 T cell lineage with regulatory T cell ties. *Immunity* 24: 677-688.
Wei FW, Hu YB, Zhu LF, Bruford MW, et al. (2012). Black and white and read all over: the past, present and future of giant panda genetics. *Mol. Ecol*. 21: 5660-5674.
Yoshimoto T, Takeda K, Tanaka T, Ohkusu K, et al. (1998). IL-12 upregulates IL-18 receptor expression on T cells, Th1 cells, and B cells: synergism with IL-18 for IFN-gamma production. *J. Immunol*. 161: 3400-3407.
Yu L, Luan PT, Jin W, Ryder OA, et al. (2011). Phylogenetic utility of nuclear introns in interfamilial relationships of Caniformia (order Carnivora). *Syst. Biol*. 60: 175-187.
Zhan XJ, Li M, Zhang ZJ, Goossens B, et al. (2006). Molecular censusing doubles giant panda population estimate in a key nature reserve. *Curr. Biol*. 16: R451-R452.
Zou J, Bird S, Truckle J, Bols N, et al. (2004). Identification and expression analysis of an IL-18 homologue and its alternatively spliced form in rainbow trout (*Oncorhynchus mykiss*). *Eur. J. Biochem*. 271: 1913-1923.